A precision measurement of the branching fraction $\mathcal{B}(\tau^\pm \to h^\pm\pi^0\nu_\tau)$ from CLEO II

Alan J. Weinstein *

California Institute of Technology
256-48 Lauritsen Laboratory
Pasadena, California 91125

Using data from the CLEO II detector at CESR, we measure $\mathcal{B}(\tau^\pm \to h^\pm\pi^0\nu_\tau)$ where $h^\pm$ refers to either $\pi^\pm$ or $K^\pm$. We use $\tau^+\tau^-$ events in which one tau decays to $h^\pm\pi^0\nu_\tau$ and the other decays into either $e^\pm\nu_e\nu_\tau$, $\mu^\pm\nu_\mu\nu_\tau$, $h^\pm\pi^0\nu_\tau$, or $h^\pm h^+h^-(\pi^0)\nu_\tau$. We use three different methods to measure this branching fraction. The combined result is $\mathcal{B}(\tau^\pm \to h^\pm\pi^0\nu_\tau) = 0.2587 \pm 0.0012 \pm 0.0042$, in good agreement with predictions from CVC. This result, in combination with other precision measurements, reduces the significance of the one-prong problem in tau decays. Preliminary results from a fit to the $\pi^\pm\pi^0$ mass distribution are also presented.

1. INTRODUCTION

The largest decay mode of the tau lepton is to one charged pion, one π^0, and a neutrino. The branching fraction for this mode is not precisely known, with measured values ranging from 22% to 26% [1,2]. Both the magnitude and shape of the $\pi^\pm\pi^0$ spectrum provide information on the charged weak spectral function and a test of the Conserved Vector Current (CVC) hypothesis. The significance of the "one-prong problem" [1,2], the gap between the inclusive one-prong branching fraction and the sum of exclusive modes, depends strongly on the magnitude and precision of the $\tau^\pm \to h^\pm\pi^0\nu_\tau$ branching fraction (referred to as the $h^\pm\pi^0\nu_\tau$ mode; $h^\pm$ refers to either $\pi^\pm$ or $K^\pm$). In addition, the CLEO measurements of the multi-π^0 ($h^\pm n\pi^0\nu_\tau$, $n > 1$) decay branching fractions [4] are normalized to the $h^\pm\pi^0\nu_\tau$ mode in order to minimize systematic errors; a precision measurement of the $h^\pm\pi^0\nu_\tau$ mode is then needed to turn those ratios into branching fractions.

In this paper we present a precise measurement of the branching fraction $\mathcal{B}_{h\pi^0} \equiv \mathcal{B}(\tau^\pm \to h^\pm\pi^0\nu_\tau)$. The $h^\pm\pi^0\nu_\tau$ mode is dominated by $\rho^\pm\nu_\tau$, but also receives contributions from $K^*\nu_\tau$, $\rho'\nu_\tau$, and non-resonant $h^\pm\pi^0\nu_\tau$ modes. This final state is referred to in this paper as the ρ mode for brevity. No attempt is made to distinguish $\pi^\pm$ from $K^\pm$ in this analysis; the charged particles are assumed to be pions.

Taus are produced in pairs at e^+e^- colliders, and the tau which recoils against the one observed to decay into $h^\pm\pi^0\nu_\tau$ is referred to as the tag. We use four different tag decay modes: $e^\pm\nu_e\nu_\tau$, $\mu^\pm\nu_\mu\nu_\tau$, $h^\pm\pi^0\nu_\tau$, and $h^\pm h^+h^-(n\pi^0)\nu_\tau$, denoted as e, μ, ρ, and 3 tag, respectively. We choose combinations of event topologies which yield the branching fraction for $h^\pm\pi^0\nu_\tau$ with minimum systematic errors and uncorrelated statistical errors. The $h^\pm\nu_\tau$ tag mode is not used because of difficulties in evaluating its trigger and $h^\pm$ identification efficiencies.

Denoting the measured number of background-subtracted, acceptance-corrected events of a given topology by, *e.g.*, $N_{\mu\rho}$ for the μ *vs.* ρ final state, we calculate the branching fraction via the following methods:

$$\mathcal{B}_{h\pi^0} = \sqrt{\frac{N_{e\rho}N_{\mu\rho}}{2N_{e\mu}N_{\tau\tau}}}, \quad \sqrt{\frac{N_{\rho\rho}}{N_{\tau\tau}}}, \text{ or } \frac{N_{3\rho}}{N_{31}}\,\mathcal{B}_1. \qquad (1)$$

These will be referred to as the $\ell-\rho$, $\rho-\rho$, and $3-\rho$ methods, respectively. The $\ell-\rho$ and $\rho-\rho$ methods normalize to the number of produced tau pairs $N_{\tau\tau}$, determined from the measured luminosity and the theoretical tau pair produc-

*Work supported by the Department of Energy under Grant DE-FG03-92-ER40701.

tion cross section, as discussed below; the $3-\rho$ method is independent of these quantities. Since the branching fraction for the first two methods is determined from the square root of the measured rates, errors associated with these rates and with $N_{\tau\tau}$ are halved. The $\ell-\rho$ method arranges the measured rates in a combination that is independent of both the leptonic decay branching fractions of the tau and the lepton identification efficiency. The $\rho-\rho$ method has no dependence on branching fractions other than the one that is being measured. The $3-\rho$ method is designed to avoid the uncertainty in the three-prong inclusive branching fraction of the tau by normalizing instead to the one-prong inclusive branching fraction $\mathcal{B}_1$. The current world average for $\mathcal{B}_1$ is [1–3] 0.852 ± 0.004. All three methods depend on understanding the absolute efficiency for reconstructing the π^0, as well as the level of background from other $\tau^+\tau^-$ topologies.

2. DATASET

The data were accumulated using the CLEO II detector [5] with the CESR e^+e^- collider at beam energy $E_b \sim 5.3$ GeV and center-of-mass energy $E_{cm} = 2E_b$. The analysis uses information from a 67-layer tracking system and a 7800-crystal CsI calorimeter, both of which are inside a 1.5 T superconducting solenoidal magnet, and a muon identification system.

A total integrated luminosity of 1.58 fb^{-1} is used for this analysis. The luminosity is measured using $e^+e^- \to e^+e^-$, $\mu^+\mu^-$, and $\gamma\gamma$ final states, observed at wide angles ($|\cos\theta| < 0.77$, where θ is the angle of the particle with respect to the e^+ beam). The absolute luminosity is determined with an error of 1% [6]. The tau pair production cross section $\sigma(\tau^+\tau^-)$ at these center-of-mass energies is calculated (to order α^3) to be 1.173 times the order α^2 cross section of $86.86/E_{cm}^2$ nb (E_{cm} in GeV), with a theoretical relative uncertainty of 1% [7]. The total number of produced tau pairs is calculated by summing the cross section times luminosity for each CLEO data run; this yields $N_{\tau\tau} = 1.440 \times 10^6$ produced tau pairs, with a systematic error of 1.4%.

3. EVENT SELECTION

The event selection and π^0 reconstruction methods are similar for all event topologies. For the $e-\mu$, $e-\rho$, $\mu-\rho$, and $\rho-\rho$ topologies, we require an event to contain exactly two charged tracks separated in angle by $> 90°$. For the $3-\rho$ and $3-1$ topologies, we require an event to contain exactly four charged tracks with three in one hemisphere (as defined by the event thrust axis). The event must have zero net charge.

All charged tracks are required to be observed in the central part of the detector ($|\cos\theta| < 0.71$ where θ is the angle of the track with respect to the e^+ beam), to be consistent with coming from the nominal e^+e^- collision point, and to have momentum greater than $0.1E_b$. Calorimeter showers are considered as candidates for photons from π^0 decays if they are observed in the central part of the detector, are not matched to a charged track, and have energy greater than 50 MeV. Pairs of photons with invariant mass within 3.5 σ of the π^0 mass (the $\gamma\gamma$ invariant mass rms resolution σ varies from 5 to 10 MeV/c^2, depending on π^0 energy) are considered as π^0 candidates. As a check, the $M_{\gamma\gamma}$ distribution is fitted to the experimentally determined line shape to extract the number of reconstructed π^0's. The energy of each π^0 is required to be greater than $0.05E_b$ or $0.10E_b$, depending on tag. Electrons and positrons are identified by requiring the energy deposited in the calorimeter to be consistent with the momentum of the charged track ($E/p > 0.8$), and the energy deposited in the drift chamber (dE/dx) to be no more than 2 σ below that expected for electrons. Muon candidates are required to penetrate $\geq$3 interaction lengths of material in the muon system.

The π^0 candidates are associated with the charged track nearest in angle, to form a $h^\pm\pi^0$ candidate. The total visible energy in the event must be greater than $0.3E_{cm}$, and the net transverse momentum in the event must exceed $0.075E_b$, to suppress background from two photon processes.

Calorimeter showers that are not matched to charged tracks or used in the ρ candidates can come from several sources, including (a) decays of π^0's from background $\tau^+\tau^-$ events with higher π^0

multiplicity ("feed-across") or from the hadronic continuum; (b) photons from initial- or final-state radiation; (c) secondary showers from hadronic interactions in the calorimeter, spatially separated from the parent, or (d) showers from detector noise or the circulating beams, but unrelated to the e^+e^- interaction. In order to suppress backgrounds from source (a), we veto events which contain additional showers having energy above 75 MeV, transverse energy profile consistent with that for photons, and >30 cm isolation from the entrance point of any charged track into the calorimeter. In the $3-\rho$ and $3-1$ topologies, extra showers are permitted in the hemisphere containing the 3-prong tag or 1-prong inclusive decay; instead, the invariant mass of all observed particles in these hemispheres is required to be less than the tau mass. Modes containing an unobserved K_L or $\omega \to \gamma\pi^0$ are considered to be $\tau^+\tau^-$ feed-across, *i.e.*, background for which a correction will be applied. The final branching fraction *does not include* such modes.

The loss of signal events due to sources (b) and (c) is estimated using a detailed simulation of the kinematics of signal topologies from the KORALB [7] Monte Carlo event generator, which generates radiative photons from $\tau^+\tau^-$ production and decay, and of the calorimeter response from a GEANT-based detector simulation package. The loss due to source (d) is simulated by merging random-trigger events from the data with Monte Carlo signal events. The veto criteria have been designed to be insensitive to the small differences between Monte Carlo and data for hadronic showers, which are more difficult to simulate than electromagnetic showers.

4. RESULTS

The number of events observed in each topology is given in Table 1. Note that the statistical error on $\mathcal{B}(\tau^\pm \to h^\pm\pi^0\nu_\tau)$ is small compared with the systematic uncertainties in our estimates of the signal reconstruction efficiencies and backgrounds. Also listed is the efficiency for reconstructing the signal topologies ($\mathcal{E}_S$), estimated from Monte Carlo simulation, and the fraction of observed events from the background (f_B). The backgrounds from $\tau^+\tau^-$ feed-across are estimated using Monte Carlo simulation and world averages [1–4] for the branching fractions of the tau to feed-across modes (dominantly from the decay $\tau^\pm \to h^\pm\pi^0\pi^0\nu_\tau$ [4] where one π^0 is not detected).

Table 1
For each event topology, we give the total number of events found, the background fraction (f_B), and the signal reconstruction efficiency ($\mathcal{E}_S$).

Topology	Events	f_B (%)	$\mathcal{E}_S$ (%)
$e-\rho$	13353	2.9	9.8
$\mu-\rho$	11758	2.9	8.9
$e-\mu$	16088	0.2	17.9
$\rho-\rho$	6498	5.9	6.5
$3-\rho$	12469	6.7	10.4
$3-1$	85959	6.2	22.3

5. SYSTEMATIC ERRORS

The efficiencies for reconstruction of signal topologies and tau-pair backgrounds receive contributions from the trigger, charged particle tracking, photon detection and π^0 reconstruction, and the effect of cuts on momenta, angles, and energies. The trigger efficiency is greater than 99% for all topologies except for $e-\mu$ and $\mu-\rho$, where the efficiency is as low as 95% for some data-taking periods. These efficiencies are measured using the data. The charged-track-finding efficiency is also near 100% for the track criteria used here; this is verified by studying independent samples of events with similar topologies. The uncertainty in the track finding efficiency is 0.5% per track. The lepton identification efficiencies and uncertainties cancel in the $\ell-\rho$ method (these uncertainties are not negligible, and precision measurements of leptonic or three-prong inclusive branching fractions cannot be obtained from the yields in Table 1). Fake lepton backgrounds are not included in f_B.

Reconstruction of π^0 decays is well simulated by the GEANT-based Monte Carlo, as seen in Fig. 1. The peak position, width, low mass tail, and background level are all well reproduced. This is quantified by varying the cuts and methods used to reconstruct photons and π^0's, and determining the change in the measured branching fraction. Imperfect knowledge of the detector material in front of the calorimeter (and hence the photon conversion rate) also contributes to uncertainty in the absolute efficiency for π^0 reconstruction.

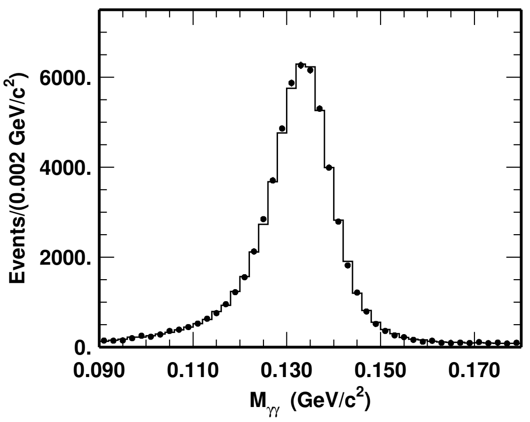

Figure 1. The $M_{\gamma\gamma}$ distribution for the data (points) and the Monte Carlo (histogram), summed over all tags.

The distributions of all kinematical quantities in the signal events are compared between data and Monte Carlo. Examples of such comparisons are shown in Figs. 2 through 4. There is good agreement in all distributions, within the accepted region, indicating that the acceptance is well modelled, and that no significant background (other than the $\tau^+\tau^-$ feed-across component included in the Monte Carlo simulation) remains in the data. Again, this is quantified by applying new cuts or varying existing ones over a wide range in acceptance, and observing the change in the measured branching fraction. We have performed several other cross-checks of our π^0 reconstruction and extra energy veto efficiency using our $\tau^+\tau^-$ data, all of which yield consistent results [8]. In no case does a cut variation produce a change in the nominal branching fraction by as much as $\pm 1\%$.

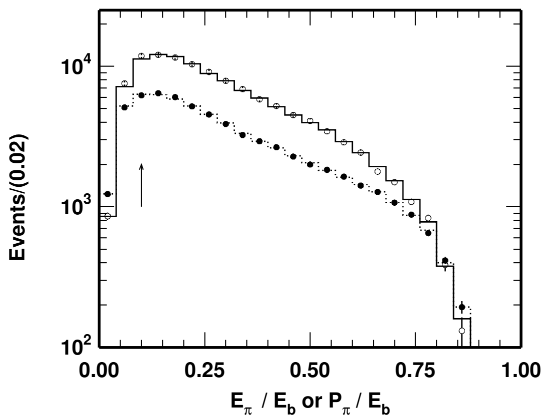

Figure 2. The distributions, summed over all tags, of the scaled momentum of the charged particles p_π/E_b, (open circles are data, solid histogram is Monte Carlo), and the scaled energy of the π^0, E_{π^0}/E_b (solid circles are data, dotted histogram is Monte Carlo, both scaled by a factor 3 for clarity). The accepted region is to the right of the vertical line.

The largest source of background in these topologies is from $\tau^+\tau^-$ feed-across events in which the $h^\pm\pi^0$ system is replaced by a system containing additional π^0's which are not observed. The sensitivity of our result to uncertainties in these branching fractions [4] is minimized by the tight veto on extra showers; f_B is small (see Table 1). Backgrounds from tau decays containing a K_L or ω meson can be estimated reliably from measured branching fractions [1,9]. Other sources of backgrounds include tau decay modes containing two spurious showers which fake a π^0; our π^0 reconstruction algorithms

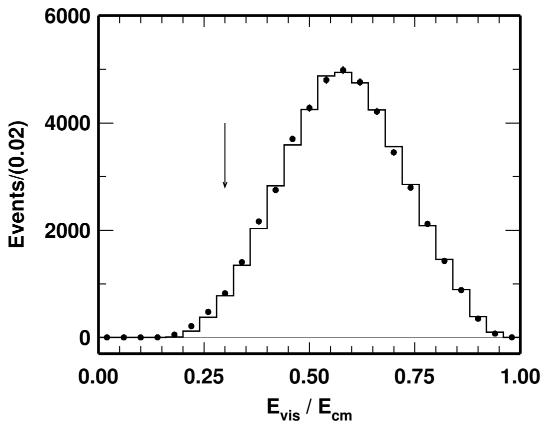

Figure 3. The scaled visible energy, E_{vis}/E_{cm}, summed over all tags (solid circles are data, histogram is Monte Carlo). The accepted region is to the right of the vertical line.

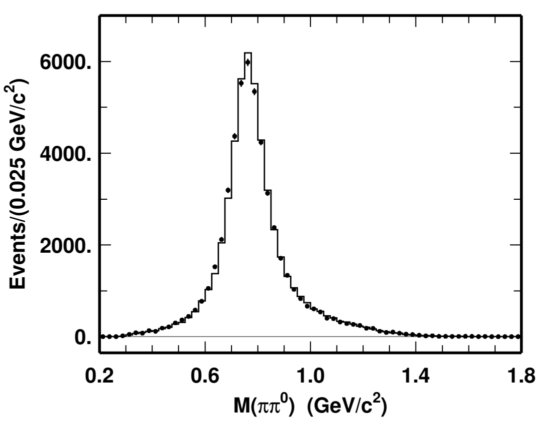

Figure 4. The $h^{\pm}\pi^0$ invariant mass, assuming $h = \pi$, summed over all tags (solid circles are data, histogram is Monte Carlo).

reduce this background to a negligible value. The backgrounds from hadronic continuum and $B\bar{B}$ production are very small except in the $3-\rho$ and $3-1$ topologies; they are estimated from the data, using events in which the invariant mass of all observed particles in the 3-prong hemisphere is greater than the tau mass [10].

The systematic errors associated with uncertainties in the signal efficiency ($\mathcal{E}_S$), the background fraction (f_B), and the number of produced tau pairs ($N_{\tau\tau}$), are tabulated for the three methods in Table 2. The largest sources of uncertainty are the absolute π^0 reconstruction efficiency, the inefficiency due to the extra shower veto, and the modelling of the inclusive 3-prong decay acceptance.

6. CONCLUSIONS

The values of $\mathcal{B}_{h\pi^0}$ determined using equation (1) are:

$$\begin{aligned}
\mathcal{B}_{h\pi^0} &= 0.2559 \pm 0.0019 \pm 0.0047 \quad (\ell-\rho);\\
\mathcal{B}_{h\pi^0} &= 0.2567 \pm 0.0017 \pm 0.0045 \quad (\rho-\rho);\\
\mathcal{B}_{h\pi^0} &= 0.2643 \pm 0.0029 \pm 0.0052 \quad (3-\rho);\\
\mathcal{B}_{h\pi^0} &= 0.2587 \pm 0.0012 \pm 0.0042 \quad (\text{comb}).
\end{aligned}$$

The combined result is obtained by weighting each measurement's statistical and uncorrelated systematic errors. Many of the largest sources of systematic errors are common to all three methods, reflected in the combined systematic error. The three measurements have a χ^2 of 2.4 for two degrees of freedom.

The $K^{\pm}\pi^0\nu_\tau$ component of our signal is obtained from an independent measurement [11] of the branching fraction $\mathcal{B}(\tau^{\pm} \to K^{\pm}\pi^0\nu_\tau) = 0.0051 \pm 0.0011$. Thus, the $\pi^{\pm}\pi^0\nu_\tau$ mode branching fraction is $\mathcal{B}_{\pi\pi^0} = 0.2536 \pm 0.0044$. This compares well with a prediction [12] derived from CVC and data on the cross section $\sigma(e^+e^- \to \pi^+\pi^-)$, $\mathcal{B}_{\pi\pi^0} = 0.2458 \pm 0.0093 \pm 0.0027 \pm 0.0050$, where the errors are from the e^+e^- data, the tau lifetime, and radiative corrections, respectively. The measured value is larger and more precise than previous measurements [1,2].

In a previous publication [4], we have presented measurements of the multi-π^0 ($h^{\pm}n\pi^0\nu_\tau$) tau decay branching fractions normalized to the $h^{\pm}\pi^0\nu_\tau$ mode. The measurement presented here can be used to convert those measured ratios to branching fractions. The resulting sum of branching

Table 2
Relative systematic errors (%), for the three methods of measuring the branching fraction.

Source of error	$\ell - \rho$	$\rho - \rho$	$3 - \rho$
trigger efficiency	0.7	0.2	0.1
tracking efficiency	0.5	0.5	0.2
π^0 reconstruction	0.9	0.9	0.9
acceptance	0.5	0.5	1.1
extra shower veto	0.9	0.9	0.9
MC statistics	0.5	0.4	0.6
$\tau^+\tau^-$ feed-across	0.3	0.4	0.7
non-τ backgrounds	0.2	0.4	0.4
luminosity	0.5	0.5	–
$\sigma(\tau^+\tau^-)$	0.5	0.5	–
$\mathcal{B}_1$	–	–	0.4
combined	1.9	1.8	2.0

fractions is

$$\begin{aligned}
\mathcal{B}(h^\pm\pi^0\pi^0\nu_\tau) &= (8.92 \pm 0.15 \pm 0.44)\% \\
\mathcal{B}(h^\pm\pi^0\pi^0\pi^0\nu_\tau) &= (1.06 \pm 0.08 \pm 0.12)\% \\
\mathcal{B}(h^\pm\pi^0\pi^0\pi^0\pi^0\nu_\tau) &= (0.15 \pm 0.05 \pm 0.05)\% \\
\mathcal{B}(h^\pm n\pi^0\nu_\tau),\ n > 0 &= (36.00 \pm 0.65)\%
\end{aligned}$$

Decay modes which include K_L and/or K_S mesons, or ω mesons in their decay $\omega \to \gamma\pi^0$, are not included in these branching fractions. When the world average values of tau branching fractions to $e^-\bar{\nu}_e\nu_\tau$, $\mu^-\bar{\nu}_\mu\nu_\tau$, $h^-\nu_\tau$, and decays involving K^0 mesons are added to this result, the one-prong problem is greatly reduced in significance.

7. PRELIMINARY MASS FITS

In order to study the $\pi^\pm\pi^0$ invariant mass distribution in the decay $\tau^- \to \pi^\pm\pi^0\nu_\tau$, we correct the observed distribution for backgrounds and detection efficiency. In this context, the the decay to $K^-\pi^0\nu_\tau$ is considered a background, in addition to the other significant backgrounds from tau decays to $h^-\pi^0\pi^0\nu_\tau$ and $h^-\pi^0K_L^0\nu_\tau$. The shape and efficiency versus invariant mass for these backgrounds are evaluated from Monte Carlo, and the normalizations are determined using world average branching fractions [1]. The resulting spectrum is shown as data points in Fig. 5. Bin migration due to detector resolution effects is small; the Monte Carlo predicts than 65% of events end up in the right bin, and 97% end up within 1 bin of the correct one.

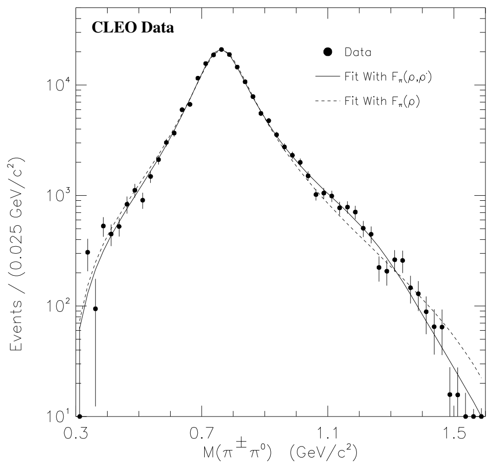

Figure 5. The distribution of $\pi^\pm\pi^0$ invariant mass, after background subtraction and efficiency correction, for the data (points). The solid line is the result of a fit described in the text, with contributions from the ρ and ρ' resonances. The dashed line is a fit with only a contribution from the ρ.

The $\pi^\pm\pi^0$ invariant mass distribution ($q^2 \equiv M^2(\pi^\pm\pi^0)$) can be related via an isospin rotation and CVC to the cross section versus $\sqrt{s}$ for $e^+e^- \to \pi^+\pi^-$. The e^+e^- cross section can be used [12] to extract the pion form factor $F_\pi(q^2)$ in the region of the ρ resonance ($q^2 \simeq (0.77\text{GeV})^2$):

$$\sigma_{e^+e^-\to\pi^+\pi^-} = \frac{\pi\alpha^2}{3q^2}\left(1 - \frac{4m_\pi^2}{q^2}\right)^{\frac{3}{2}} |F_\pi(q^2)|^2.$$

The form factor extracted in this way is well described by a sum of interfering resonances, associated with the $\rho(770)$, $\omega(792)$, and a higher mass state taken to be a $\rho'(1450)$. The $\omega(782)$ component is isoscalar and thus does not contribute to tau decay. Taking only the isovector part of the form factor, $F_\pi^{I=1}(q^2)$, we can model the $\pi^\pm\pi^0$ invariant mass distribution in τ decay as:

$$\begin{aligned}\frac{d\Gamma}{dq}(\pi\pi^0\nu_\tau) &= \frac{G_F^2 m_\tau^5}{384\pi^3}|V_{ud}|^2 \\ &\times\frac{2q}{m_\tau^2}\left(1-\frac{q^2}{m_\tau^2}\right)^2\left(1+2\frac{q^2}{m_\tau^2}\right) \\ &\times\left(1-\frac{4M_\pi^2}{q^2}\right)^{\frac{3}{2}}|F_\pi^{I=1}(q^2)|^2.\end{aligned}$$

Following Ref. [12], we adopt the form

$$F_\pi^{I=1}(q^2) = (BW_\rho(q^2) + \beta BW_{\rho'}(q^2))/(1+\beta),$$

where BW_R is a relativistic Breit Wigner resonance lineshape with mass-dependent width, normalized to 1 at $q^2=0$.

We have made preliminary fits to the $\pi^\pm\pi^0$ invariant mass distribution using the above form, extracting values for the masses and widths of the ρ and ρ' resonances, and for the parameter β. The fit result is shown as the solid line in Fig. 5, which yields a χ^2 of 64 for 46 degrees of freedom. There is clear evidence for a ρ' resonance, as a distortion of the high-mass tail of the ρ. The parameter β is 6σ from zero. We achieve statistical errors of 1 MeV/c^2 for the mass of the ρ, 1 MeV for its width, 17 MeV/c^2 for the mass of the ρ', and 60 MeV for its width. Fits to Monte Carlo spectra show that these parameters can be measured with systematic errors on the same order as the statistical errors; these are currently being evaluated. The results are in good qualitative agreement with the e^+e^- fit results [12], providing a clean test of CVC. The $\pi^\pm\pi^0$ pseudo-helicity angle distribution is also under study.

In conclusion, we have presented a high-precision measurement of the branching fraction for the decay $\tau^\pm \rightarrow h^\pm\pi^0\nu_\tau$. We have employed four tagging decays, in three statistically independent combinations, which are in good agreement with each another. Common systematic errors limit the overall precision to $\sim 1.7\%$ [8]. A preliminary analysis of the $\pi^\pm\pi^0$ invariant mass spectrum shows good agreement with CVC predictions.

8. ACKNOWLEDGEMENTS

We gratefully acknowledge the effort of the CESR staff in providing us with excellent luminosity and running conditions. I gratefully acknowledge the effort of the Tau94 staff in providing us with excellent surroundings, accommodations, meals, and stimulating conversation.

REFERENCES

1. L. Montanet *et al.* (Particle Data Group), Phys. Rev. **D50**, 1 (1994).
2. See the review by Brian Heltsley in these proceedings.
3. We assume that the one-prong branching fraction $\mathcal{B}_1$ excludes modes containing $K_S \rightarrow \pi^+\pi^-$ decays; the systematic error on $\mathcal{B}_1$ is increased to account for this ambiguity.
4. M. Procario *et al.* (CLEO Collaboration), Phys. Rev. Lett. **70**, 1207 (1993).
5. Y. Kubota *et al.* (CLEO Collaboration), Nucl. Instr. Methods **A320**, 66 (1992).
6. G. Crawford *et al.* (CLEO Collaboration), Nucl. Instr. Meth. A345 (1994) 429.
7. KORALB (v.2.1) and TAUOLA (v.1.5): S. Jadach and Z. Was, Comput. Phys. Commun. **36**, 191 (1985) and *ibid*, **64**, 267 (1991); S. Jadach, J.H. Kühn, and Z. Was, Comput. Phys. Commun. **64**, 275 (1991), *ibid*, **70**, 69 (1992), *ibid*, **76**, 361 (1993).
8. Further details on the systematic errors, and studies of the $\pi^\pm\pi^0$ invariant mass and decay angle distributions, will be presented in a future publication.
9. See the contribution by Jim Smith in these proceedings.
10. The method is described in D. Bortoletto *et al.*, Phys. Rev. Lett. **71**, 1791 (1993).
11. M. Battle *et al.*, CLNS 94/1273 (1994), submitted to Phys. Rev. Lett.
12. J. Kühn and A. Santamaria, Z. Phys. **C48**, 443 (1990); W. Marciano, in *Proceedings of the Second Workshop on Tau Lepton Physics*, September 1992, ed. K.K. Gan, World Scientific (1993).